International Journal of the Physical Sciences Vol. 7(4), pp. 534 - 543, 23 January, 2012
Available online at http://www.academicjournals.org/IJPS
DOI: 10.5897/IJPS11.1019
ISSN 1992 - 1950 © 2012 Academic Journals

Full Length Research Paper

The effect of magnetic field and nanofluid on thermal performance of two-phase closed thermosyphon (TPCT)

S. Zeinali Heris[1,2]*, H. Salehi[1,2] and S. H. Noie[1,2]

[1]Department of Chemical Engineering, Faculty of Engineering, Ferdowsi University of Mashhad, Mashhad, Iran.
[2]Heat Pipe and Nanofluid Research Center, Faculty of Engineering, Ferdowsi University of Mashhad, Mashhad, Iran.

Accepted 3 January, 2012

The efficiency of two-phase closed thermosyphon (TPCT) with nanofluid as working fluid under magnetic field effect was investigated experimentally. In this study, silver/water nanofluid with different concentration (20 to 80ppm) is tested. Also, magnetic field with various strength (0.12, 0.35 and 1.2 T) exerted to TPCT by permanent magnet. It was seen that the TPCT heat transfer performance and the thermophysical properties of the base fluid are considerably affected by the nanoparticles addition and magnetic field. According to the experimental result, the thermal efficiency of thermosyphon significantly increased with the nanoparticles concentration increasing as well as magnetic field strength, and the TPCT shows better performance in the highest value of concentration (80 ppm) and magnetic field (1.2 T). Moreover, the experimental results represent that thermal efficiency in the presence of magnetic field somewhat increases.

Key words: Silver/water nanofluid, permanent magnet, two phase closed thermosyphon, thermal efficiency, heat transfer enhancement, magnetic field.

INTRODUCTION

The new technological developments as well as the industrial process intensification have made the need for more efficient heat exchanging systems a contemporary demand. Therefore, the scientific interest is focused both on improving the equipment design and on enhancing the thermal capability of the working fluids. Most commonly used working fluids in heat exchangers are water, methanol, ethylene glycol and oil which are originally poor heat transferring fluids. Numerous techniques have been introduced to improve the thermal performance of these fluids. Consequently, fluids with nanosized particles suspended in them which are later called nanofluids have been proposed by Choi (1995). Nanofluids are also well known in production of nanostructured materials (Tseng and Wu, 2002), engineering of complex fluids (Tohver et al., 2001) as well as enhancement of wetting and spreading behavior (Wasan and Nicolov, 2003).

Kim et al. (2006) investigated the effects of thermo-diffusion and nanoparticles on convective instabilities in binary nanofluids, and indicated that the Soret effect of solute that dissolved in binary nanofluids makes binary nanofluids unstable. Also, from their results, it can be found that the heat transfer enhancement by the Soret effect in binary nanofluids is more significant than that in normal nanofluids. Kang et al. (2006) investigated the thermal conductivities of silica, silver and ultra-dispersed diamond (UDD) nanoparticles suspension. The experimental results show that thermal conductivity enhancement was up to 70% for the best case of 1% UDD in ethylene glycol. In order to estimate the exact thermal conductivity, they used the effective particle volume fraction which was estimated by the measurement of viscosity. Their results show that heat transfer mechanisms, such as phonon transport in the solid/liquid interface and electron transport, must be considered to estimate the exact thermal conductivity of nanofluid. The mechanism of heat transfer intensification, recently brought about by

*Corresponding author. E-mail: zeinali@ferdowsi.um.ac.ir. Tel: (+98) (511) 8816840. Fax: (+98) (511) 8816840.

nanofluids is analyzed by Quaresma et al. (2010) in the light of the non-Fourier dual-phase-lagging heat conduction model. The mathematical formulation for this problem is analytically solved with the classical integral transform technique, thus providing benchmark results for the temperature predicted with the dual-phase-lagging model.

Zeinali et al. (2007) numerically studied laminar fully developed convective heat transfer of a nanofluid through a circular tube with constant wall temperature boundary condition. They used the dispersion model, in which the effect of random movement of nanoparticles inside the liquid is considered as excess terms in the heat transfer equation. Model predictions have clearly revealed that addition of nanoparticles to the base fluid produces remarkable increase in heat transfer coefficients as compared to the base fluid. The results obtained by numerical solution show that increasing nanoparticle size decreases Nusselt number at a specific concentration. Yu et al. (2008) in their review paper, illustrated that the nanofluid development and manufacturing is still considered to be in the research stage, and many factors need to be optimized before commercial application. Problems of nanoparticles agglomeration, settling and erosion potential, all need to be addressed in detail. Kulkarni et al. (2008) during investigation of SiO_2 ethylene glycol/water nanofluid indicated that the viscosity of nanofluids decreases with nanoparticles size increasing, also, heat transfer coefficients of nanofluids increase with volume concentration.

Duursma et al. (2009) used spray cooling in cooling of electronic devices to remove large heat fluxes. The effect of nanoparticles on droplet boil-off was studied in their work. Increasing nanoparticles concentration decreases the receding droplet breakup on rebound after impingement and appears to reduce the maximum spreading of a droplet as well. Experimental measurements of the heat fluxes associated with the pure and nanofluid droplets did not show significant enhancement, though there was noticeable improvement in the nanofluids. Zeinali et al. (2009) experimentally investigated Cu/water nanofluid laminar convective heat transfer performance in a circular tube with constant wall boundary condition. Based on experimental results, the heat transfer coefficient was influenced by Peclet number, as well as Cu nanoparticles volume concentrations. It seems that there is an optimum concentration for Cu nanoparticles in water, in which better enhancement for heat transfer can be found.

Critical heat flux of TiO_2/water and Al_2O_3/water nanofluids in pool boiling is studied by Kim et al. (2007). Research of mechanisms of thermal nanofluids on enhanced critical heat flux is carried out by Wen (2008). His results showed that the structural disjoining pressure can significantly increase the wettability of the fluids and inhibit the dry patch development. Zhu et al. (2010) studied thermal physics and critical heat flux characteristics of Al2O3/water nanofluids. It found that a significant enhancement in critical heat flux (CHF) could be achieved at modest nanoparticles concentrations. Compared to CHF of pure water, an enhancement of 113% over that of nanofluids was found. Scanning electron microscope photos showed that there was a nanoparticles layer formed on the heating surface for nanofluid boiling. The coating layer makes the nucleation of vapor bubbles easily formed.

Two-phase closed thermosyphon (TPCT) is a high performance heat transfer device which is used to transfer a large amount of heat at a high rate with a small temperature difference. Many studies have been done to improve the efficiency and thermal performance of thermosyphon. di Francescantonio et al. (2008) studied the Marangoni effect and heat transfer enhancement of new alcohol solutions as binary mixtures with a non-linear dependence of the surface tension with temperature for heat pipes. Chang et al. (2008) experimentally investigates the thermal performance of the heat pipe cooling system with the thermal resistance model. The result shows that the evaporation resistance and the condensation resistance both grow with increasing heating power and decreasing fill ratio. Flooding phenomenon is caused by the opposite flow direction of vapor and liquid in a closed two-phase system.

Some researchers have used nanofluid as thermosyphon working fluid and have studied the thermal performance of TPCT using nanofluid (Lin et al., 2008; Coursey and Kim, 2008; Khandekar et al., 2008; Kang et al., 2009; Naphon et al., 2009). The effect of silver nanofluid on pulsating heat pipe thermal performance is studied by Lin et al. (2008). Coursey and Kim (2008) studied the effect of surface wettability on nanofluid boiling. Khandekar et al. (2008) have studied thermal performance of a close two-phase thermosyphon charged with nanofluids and observed that nanofluids show inferior thermal performance than pure water. Kang et al. (2009) experimentally investigated 10 to 35 nm Ag/water nanofluids on sintered circular heat pipe. With the same loading volume, they showed that the temperature difference between two ends of heat pipe with nanofluid decreased 0.56 to 0.65°C as compared to pure water. Naphon et al. (2009) have used refrigerant/nanoparticles nanofluid as working fluid in a heat pipe, and stated that at optimum condition for pure refrigerant, the heat pipe with 0.1% concentration of nanoparticles operates with efficiency 1.40 times higher than that with pure refrigerant.

Yang et al. (2009) studied performance characteristics of pulsating heat pipes as integral thermal spreaders. Khandekar et al. (2009) studied the multiple quasi-steady states in a closed loop pulsating heat pipe. Noie et al. (2009) studied heat transfer enhancement using Al_2O_3/water nanofluid in a two-phase closed thermosyphon. Based on experimental results, they expressed that for different input powers, the efficiency of the TPCT increases up to 14.7% when Al_2O_3/water nanofluid was

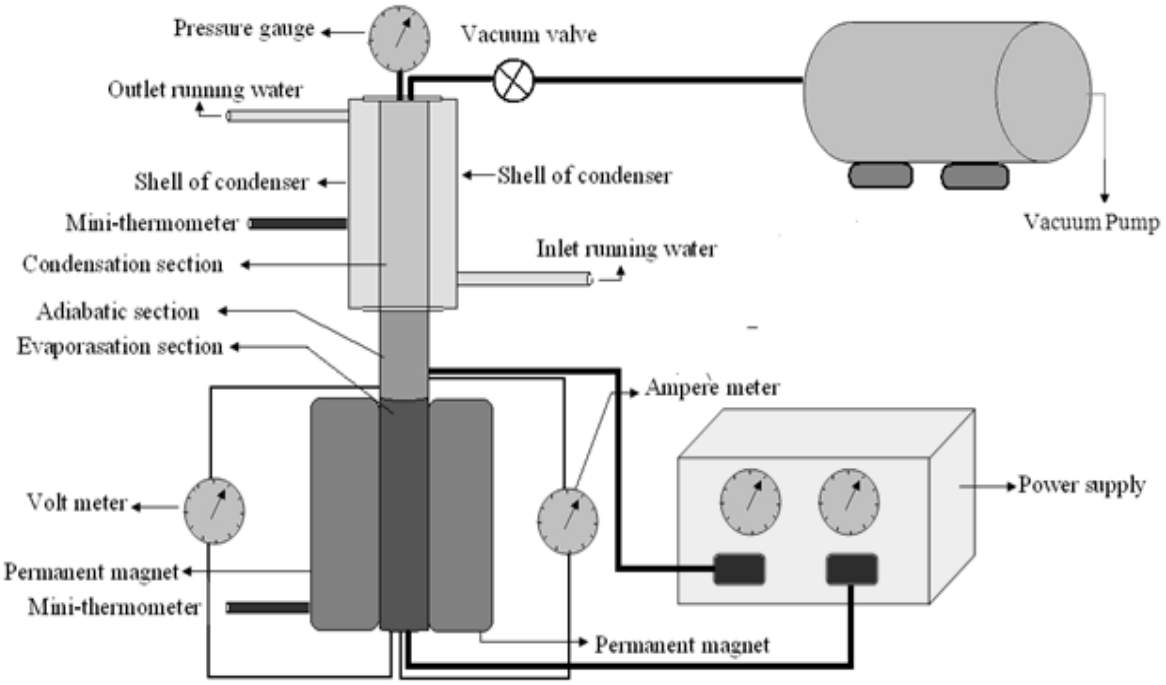

Figure 1. Schematic of experimental test rig.

used instead of pure water. Kang et al. (2006) used 10 and 35 nm Ag/water nanofluid as working fluid on heat pipe and represent the thermal enhancement of heat pipe performance adding silver nanoparticles to pure water, but the results indicated that the thermal resistances of heat pipe decrease as the Ag nanoparticles size and concentration increase.

One of the simplest ways to provide additional body force to a working fluid and heat transfer enhancement is magnetic force. Quantitative treatment of fluid convection under magnetic fields was initiated by Bai et al. (1999). Braithwaite et al. (1991) used magnetic fields both to enhance and suppress the Rayleigh-Benard convection in a solution of gadolinium-nitrate, and showed that the effect depends on the relative orientation of the magnetic force and the temperature gradient. Jeyadevan et al. (2005) evaluated the performance of heat pipe using citric ion-stabilized magnetic fluid as working fluid. Fornalik et al. (2006) studied convection of a para-magnetic fluid inside a vertical cylinder placed in the bore of a superconducting magnet. Fukuzawa and Fuji, (1978) experimentally investigated influence of transverse mag-netic field on heat transport characteristics of potassium heat pipe. Kaneda et al. (2002) presented the induction of magnetic convection in stably stratified air in a cube heated from above and cooled from below. They found that without a magnetic field, the conduction was stable, but under the magnetizing force, a strong downward flow occurred from the center of the top heated plate. Maki et al. (2002) applied magnetizing force for natural convection of air in a shallow cylindrical enclosure heated from below and cooled from above. The average Nusselt number were enhanced about twice at the location +66 mm above the coil center under 3.40 Tesla (T) and decreased to Nu = 1.12 to 1.28 at the location -66 mm below the coil center for the Rayleigh number from 3520 to 6980. A model equation for magnetizing force was derived and numerically computed for Pr = 0.7 and Ra = 2100 and 7000. Salehi et al. (2011) investigated the TPCT thermal resistance and Nusselt number ratio using CuO/water nanofluid as the working fluid under magnetic field. They expressed that although, Nusselt number in the presence of magnetic field was somewhat increased, but the experimental results indicated that the TPCT heat transfer rate is better enhanced through nanofluid concentration increment as compared to magnetic field strength enhancement.

In the present study, the effect of magnetic field strength and Ag/water nanofluid concentration as working fluid on the two-phase closed thermosyphon heat transfer performance was investigated experimentally.

EXPERIMENTAL SETUP

Figure 1 shows the schematic of experimental set up. As shown, the test rig consists of a heater, condenser for cooling the condensation section, two parallel plates of permanent magnet and also, measuring instruments. Working fluid are pure water and Ag/water nanofluid. Various concentrations of silver nanoparticles in distilled water have been used (20, 40, 60 and 80 ppm). Physical

Table 1. Different parts of thermosyphon.

Thermosyphon part	Characteristics
Long copper tube	0.40 mm l, 20 mm ID, 22 mm OD
Evaporator sections	0.20 m total length, can varied by varying the length of the electrical resistance
Adiabatic sections	0.05 m total length
Condenser section	0.15 m long, 45 mm OD

properties of nanoparticles were taken from the manufacturer data sheet (density ρs = 10490 kg/m^3, heat capacity Cps = 232 J/kg.K, thermal conductivity Ks = 429 W/m.K).

A mechanical vacuum pump capable of up to -0.9 bar and pumping capacity of 142 lit/min was used for partial elimination of the non-condensable gases from the thermosyphon. Figure 1 shows the detail of experimental apparatus. The thermosyphon consisted of a 400 mm long copper tube having an inside diameter of 20 mm and outside diameter of 22 mm. The tube was sealed at one end and was provided with a vacuum valve at the other. Table 1 represents the different parts of thermosyphon. The condenser section of the pipe consisted of a 0.15 m long (45 mm outside diameter (OD)) concentric tube acting as running water jacket surrounding the pipe. An electrical resistance of a nominal power 250 W, which was wrapped around the evaporator section, heated the evaporator section. To prevent heat loss, the electric elements were insulated by Rock Wool having a thickness of 20, 10 and 20 mm in vaporization, adiabatic and condensation section, respectively. The power supplied to the evaporator section was determined by monitoring the applied voltage and ampere. Running water inlet and outlet temperatures were measured using digital mini-thermometer with an accuracy ± 0.1°C. The flow rate of cooling water was 200 ml/min. The nanofluid was charged into the tube under -0.9 bar relative vacuum pressure. The mini-thermocouples were mechanically attached to the surface of the pipe. Permanent magnets (0.12, 0.35 and 1.2 T) are placed on the vaporization section. All the electrical (such as thermocouples, thermometers, ammeter and voltmeter) and mechanical equipments (such as rotameter) were calibrated initially.

DATA PROCESSING AND TEST PROCEDURE

The rate of heat transfer to the evaporator section was calculated from the following relation (Noie, 2005):

$$Q_{in} = VI \quad (1)$$

In Equation 1, the heat loss by radiation is neglected because of very small amount of it in low temperature. The free convection heat transfer rates to the outside atmosphere has been calculated and due to the thickness and heavy insulation of fiberglass blanket, this quantity has been neglected, because it has very small amount. The total heat loss was about 2.5% of the input power to the evaporator section.

The rate of heat removal from the condenser section was obtained from the following relation (Noie, 2005):

$$Q_{out} = \dot{m} C_p (T_o - T_i) \quad (2)$$

Also, Nusselt number was obtained from the following relation (Maki et al., 2002; Salehi et al., 2011):

$$Nu = \frac{Q_{net,conv}}{Q_{net,cond}} \quad (3)$$

In the present study, for calculating output heat transfer, we ignore the effect of heat conduction, therefore we obtain:

$$Q_{out} = Q_{net,conv} = \dot{m} C_p (T_o - T_i) \quad (4)$$

$$Q_{net,cond} = \frac{\pi}{4} d^2 k \frac{\Delta\theta}{l} \quad (5)$$

In Equation 5, $\Delta\theta$ is the temperature difference between condensation and vaporization section, k is thermal conductivity of working fluid of the thermosyphon, d and l are diameter and length of the thermosyphon, respectively.

Therefore:

$$Nu = \frac{\dot{m} C_p (T_o - T_i)}{\frac{\pi}{4} d^2 k \frac{\Delta\theta}{l}} \quad (6)$$

Thermal resistance that was obtained from the following relation (Khandekar et al., 2008):

$$R = \frac{\Delta\theta}{Q_{in}} \quad (7)$$

Also, thermal efficiency of heat pipe is calculated (Noie et al., 2009):

$$\eta_{th} = \frac{Q_{out}}{Q_{in}} \quad (8)$$

Test procedure began by charging distilled water and Ag/water nanofluid with different concentration as working fluid. The evaporator filling ratio inside thermosyphon was 40% in all experiments. Experiments were carried out with increasing input heat in the range of 12 < Q < 40 W to the evaporator section. The measured temperature of condenser section wall was 21.5°C for 12 W, 22°C for 24 W and 23°C for 40 W input power. After 30 to 40 min, when the system reached the steady state, data was recorded.

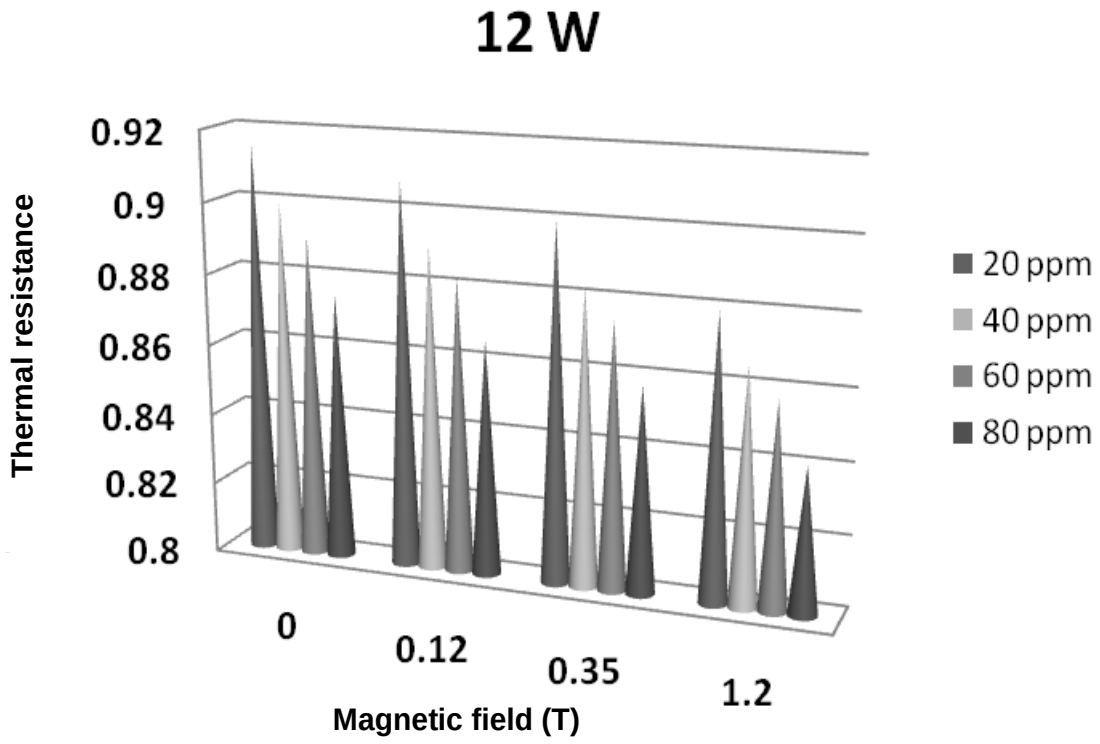

Figure 2. Effect of magnetic field on the thermal resistance for 12 W.

The hot and cold wall temperatures and mass flow rate of running water were measured to provide the thermal resistance. It is noted that the mass flow rate of running water was 200 g/min constant during experiments. Also, inlet and outlet temperatures of running water were measured to provide the rate of heat removal from condenser section, and calculate the TPCT Nusselt number. After completing the experiments in the absence of magnetic field, the permanent magnetic was changed from 0 to 1.2 T and the magnetic field was applied to the system. After 15 to 20 min, when the system reached the steady state, procurers were repeated.

Uncertainty of the experimental data may have resulted from measuring errors of parameters, such as current, voltage, inlet and outlet temperature of the cooling water, and mass flow rate, and can be calculated using the following relations for analysis of experimental uncertainty (Holman, 1989):

$$Max\,E_R = \pm\left[\left(E_{\Delta\theta}\right)^2 + \left(-E_{Qin}\right)^2\right]^{0.5} \quad (9)$$

$$Max\,E_{Nu} = \pm\left[\left(E_{Qout}\right)^2 + \left(-E_{Q_{net,cond}}\right)^2\right]^{0.5} \quad (10)$$

$$Max\,E_{Q_{net,cond}} = \pm\left[2\left(E_d\right)^2 + \left(-E_{\Delta\theta}\right)^2 + \left(E_{k_{nf}}\right)^2 + \left(-E_l\right)\right]^{0.5} \quad (11)$$

$$\mathrm{Max\ E_{Q\,out}} = \pm\left[\left(\mathrm{E_m}\right)^2 + \left(\mathrm{E_{Cp}}\right)^2 + \left(\mathrm{E_{(T_{out}-T_{in})}}\right)^2\right]^{0.5} \quad (12)$$

$$\mathrm{Max\ E_{Q\,in}} = \pm\left[\left(\mathrm{E_V}\right)^2 + \left(-\mathrm{E_I}\right)^2\right]^{0.5} \quad (13)$$

The thermocouples used have a maximum precision of 0.1°C. Flow rates were measured directly from the time taken to fill a glass vessel of known volume, with 5.0% uncertainty in measurement. The maximum precision of the ammeter and voltmeter was 0.1 V and 1 A, respectively. The maximum uncertainty of thermal resistance and Nusselt number is 4.5 and 3.5%, respectively using aforementioned relations.

EXPERIMENTAL RESULTS

Figure 2 shows the thermal resistance of TPCT versus magnetic field for various concentrations of nanofluid at input power of 12 W. It was recognized that the resistance decreases as strength of magnetic field increase. Also, thermal resistance decreases as concentration of silver nanoparticles increase. For example, at 0.35 T, the resistance of thermosyphon decreased 3.22% using 20 ppm of silver/water nanofluid as compared to pure water, but at 1.2 T and the same concentration of Ag/water nanofluid, the resistance decrease was 5.37%.

Figure 3 shows the thermal resistance of TPCT versus magnetic field for various concentrations of nanofluid at input power of 24 W. It was understood that the resistance decreases with magnetic field strength increasing as well as Ag/water nanofluid concentration increasing. For example, at 0.12 T, the resistance of thermosyphon decreased by 2.38% using 40 ppm of silver nanoparticles in pure water, but at 1.2 T, the resistance decrease was

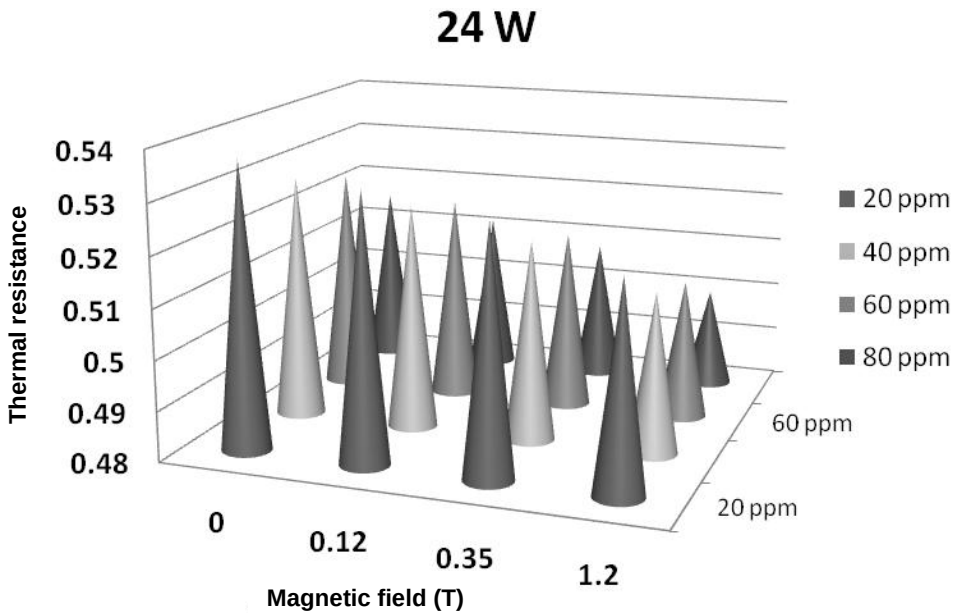

Figure 3. Effect of magnetic field on the thermal resistance for 24 W.

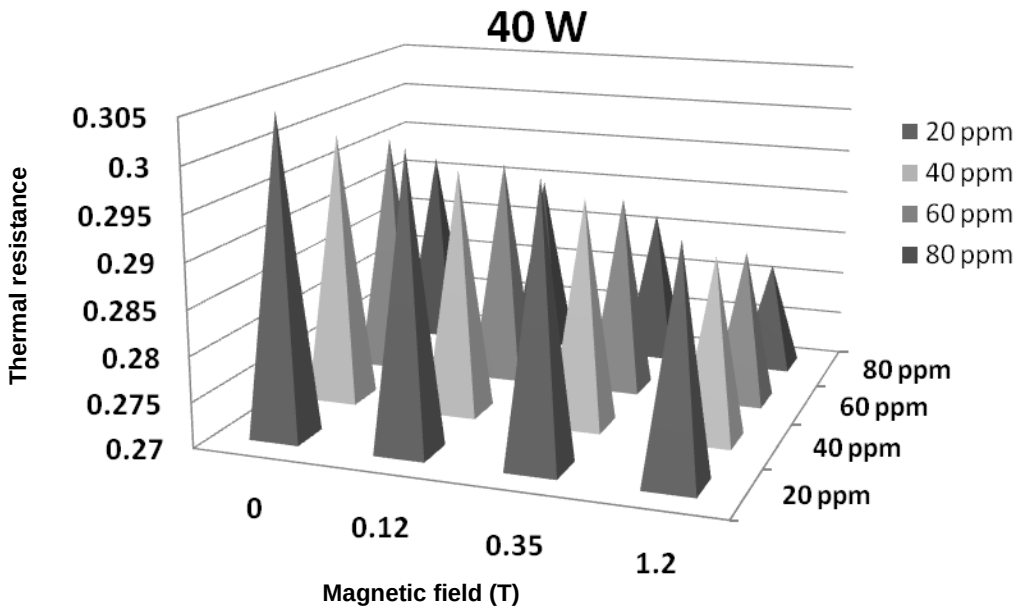

Figure 4. Effect of magnetic field on the thermal resistance for 40 W.

4.57% as compared to water with no Ag nanoparticles added to it.

Similar to Figures 2 and 3, Figure 4 shows the thermal resistance of TPCT versus magnetic field for various concentrations of nanofluid, but input power is higher than the aforementioned tests, and is 40 W. The same results obtained from Figures 2 and 3 could be found here and it was recognized that the resistance decreases as strength of magnetic field increases. Also, thermal resistance decreases as concentration of silver nanoparticles increase. For example, at 0.12 T, the resistance of thermosyphon decreased by 2.58% using 20 ppm of silver nanoparticles in pure water, but at 1.2 T, the resistance decrease was 4.83%. The comparison between Figures 2 to 4 represent that the thermal resistance of TPCT decreased with input power increasing, but the effect of nanofluid and magnetic field strength on TPCT thermal resistance decrement decreased as compared to

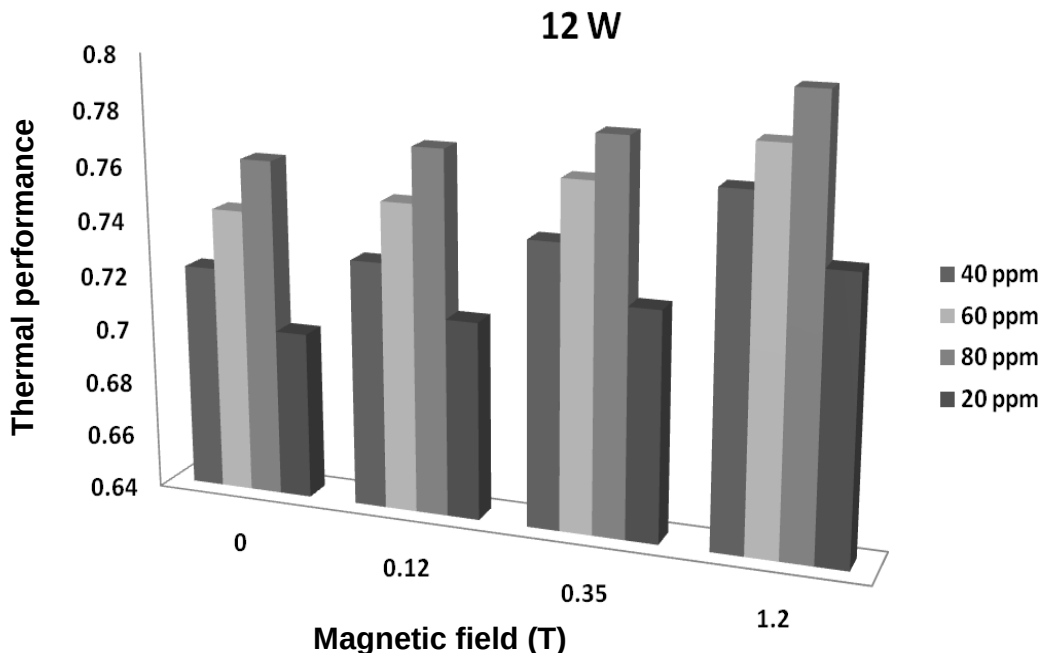

Figure 5. Effect of magnetic field on the thermal efficiency for 12 W.

pure water by increasing input power.

To interpret the thermal resistance decreasing with nanofluid concentration increasing, it may be said that the total thermal resistance of a TPCT between evaporator and condenser section consisted of thermal resistance in the heat pipe wall, the thermal resistance due to evaporation and condensation (evaporator and condenser sections) and the thermal resistance in the two-phase flow through heat TPCT length. The wall thermal resistance is independent of the working fluid. Thermal resistances at the evaporator and condenser sections were influenced by several parameters, such as surface condition of heat pipe inner wall. Generally, the bubble formation is related to the surface wettability and roughness. It is cleared from previous study about nanofluid boiling (Kim et al., 2007; Wen, 2008; Zhu et al., 2010; Coursey and Kim, 2008; Khandekar et al., 2008; Noie et al., 2009; Mikic and Rohnesow, 1969; Narayan et al., 2007; Li et al., 2008; Kim et al., 2007) that the nanoparticles changed the surface condition of the evaporator section. The sizes of nanoparticles are smaller than the cavities of the clean surface. Then, the Ag nanoparticles that may deposit on nucleation sites could create more new active nucleation sites by splitting a single nucleation site into multiple ones and enhanced the boiling heat transfer. Beside this, the irregular nanopores formed between deposited Ag nanoparticles would affect the bubble diameter and release frequency, and then bubbles may be continuously generated. Considering previous study in the literature about nanofluid and boiling heat transfer performance, one can be found that thermal resistance at evaporator section decreased because of increasing liquid thermal conductivity, density, active nucleation site density, bubble release diameter and frequency (Mikic and Rohnesow, 1969; Narayan et al., 2007; Li et al., 2008; Kim et al., 2007). The effect of nanoparticles on two-phase flow heat transfer enhancement may be illustrated through two reasons, the suspended nanoparticles increased the thermal conductivity of base fluid and the interactions among the nanoparticles itself on one hand and between nanoparticles and the inner surface of the heat pipe on the other hand, also, the diffusion and collision intensification of nanoparticles in nanofluid near duct wall due to increase in concentration of nanoparticles leads to rapid heat transfer from heat pipe wall to nanofluid.

In order to examine the effect of strength magnetic field on thermal efficiency of thermosyphon, the experimental results were plotted in Figures 5, 6 and 7 for 3 different input powers. Figure 5 shows the thermal efficiency of TPCT against magnetic field for various concentrations of nanofluid at input power of 12 W. It was found that the thermal efficiency for strength magnetic field of 1.2 T was the highest among other strength magnetic fields for input power 12 W. For example, at 0.12 T and 20 ppm of Ag/water nanofluid, the thermal efficiency of TPCT is 70%, but for 1.2 T magnetic field strength and the same concentration, the efficiency increased to 74%. The better enhancement available at higher Ag/water nanofluid concentration, so at 0.12 T and 80 ppm the efficiency is 75% and at 1.2 T and 80 ppm the thermal efficiency will be 80%.

The thermal efficiency of TPCT versus magnetic field

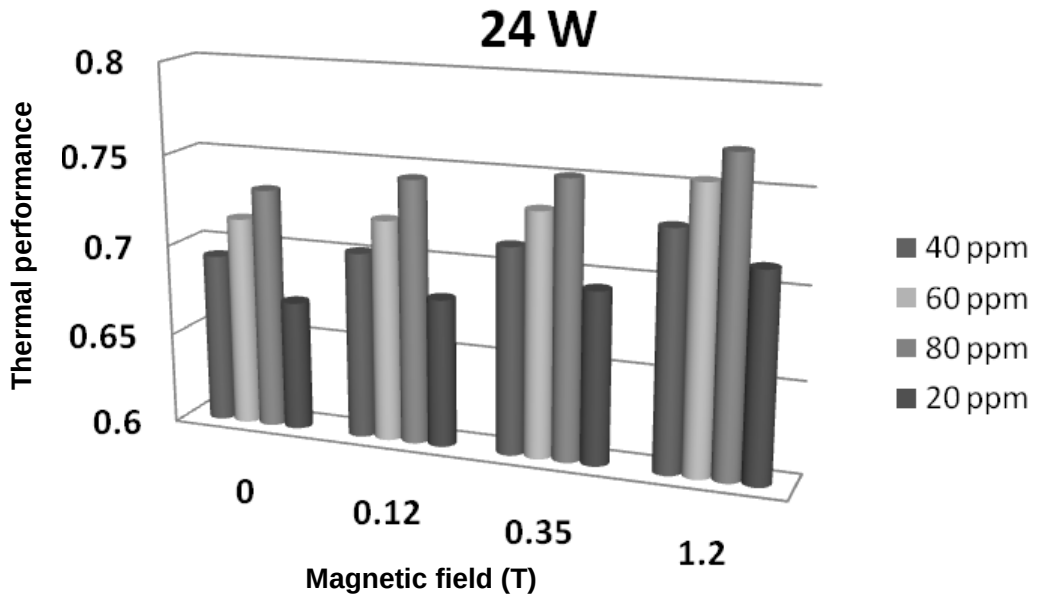

Figure 6. Effect of magnetic field on the thermal efficiency for 24 W.

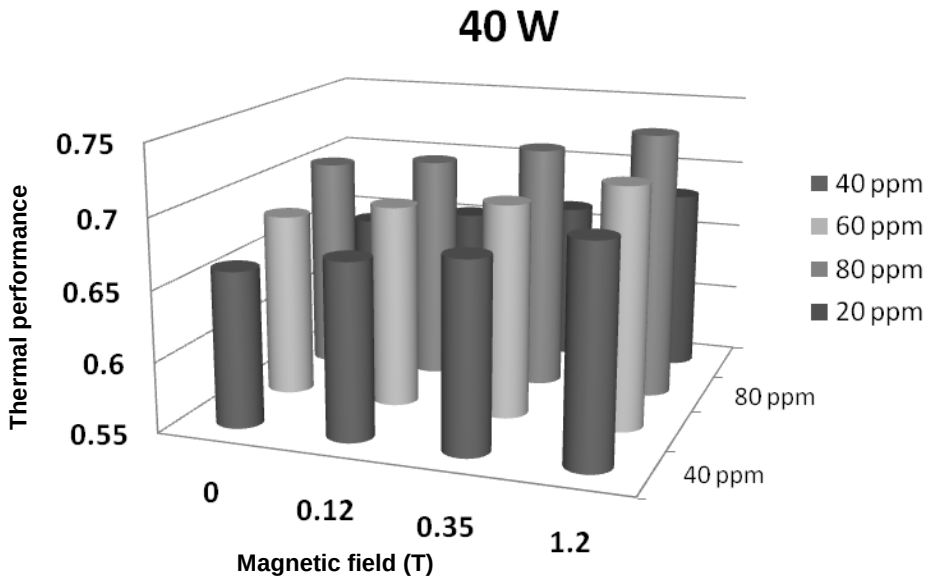

Figure 7. Effect of magnetic field on the thermal efficiency for 40 W.

for various concentrations of nanofluid at input power of 24 W is presented in Figure 6. As it is shown, for example, at 0.12 T, the thermal efficiency is about 68.1% by using 20 ppm of silver nanoparticles, but at 0.35 T, the thermal efficiency for 20 ppm of Ag/water nanofluid is about 69.4%. Also, at 80 ppm concentration, the efficiency is 73% for 0.12 T and for 1.2 T and same concentration the efficiency increases to 77%.

In order to evaluate the effect of magnetic field strength effect and nanofluid concentration on TPCT thermal efficiency at higher input power. Figure 7 presents the thermal efficiency against the magnetic field for various concentrations of nanofluid at input power of 40 W. It was recognized that the thermal efficiency improves as strength magnetic field increases. For example, at 0.35 T, this parameter is 66.5% by using 40 ppm of silver nanoparticles in pure water, but at 1.2 T, it is 67.7%. Although, the thermal resistance of TPCT decreases with input power increasing, it was found from the comparison between Figures 5 and 7, that the TPCT

thermal efficiency decreases with input power increasing because of the different effect of input power on evaporator and condensation section and also cooling water temperature.

It can be concluded that the causes of the thermal resistance decrement and efficiency increment are magnetic field and nanofluid. Because of the presence of nanoparticles in the fluid, the thermal conductivity increases which results in the improvement of total heat transfer coefficient and increase Nusselt number, and therefore, thermal resistance reduces. The effects of magnetic field on thermosyphon performance are simplified in following ways:

1. Release the bubbles which accumulated on the inner wall of evaporator;
2. Reduce temperature fluctuation in the evaporation section;
3. Reduction of temperature difference between the fluid and wall; consequently, occurring critical heat flux shorter time;
4. Increase of vapor movement due to Lorentz force.
5. Increase of liquid turbulence in evaporator dump.

In the case of up moving the nanoparticles through thermosyphon nanofluid media, the magnetic field effects caused them to rotate in fluid and also leads to entropy accretion of particles in the presence of magnetic field. The rotation of nanoparticles in water created small wakes inside the fluid and as a result, the heat transfer is enhanced. It is clear that fluid regime in thermosyphon is still laminar and application of these values of magnetic field cannot change this regime. The applied magnetic field on thermosyphon nanofluid release the bubbles which was accumulated on the inner wall of evaporator, reduce temperature fluctuation in the evaporation section, reduction of temperature difference between the fluid and wall and increase of vapor movement due to Lorentz force, then consequently, enhanced thermal efficiency of thermosyphon.

Conclusion

In this investigation, the thermal performance of two-phase closed thermosyphon using Ag/water nanofluid as the working fluid under magnetic field was studied. The thermal resistance of the thermosyphon with the silver nanoparticles suspension under magnetic field was lower than the absence of magnetic field and pure water. Also, application of magnetic field increases the thermal efficiency in the thermosyphon. It is concluded that TPCT heat transfer enhancement by nanofluid under magnetic field depends on several factors including increment of thermal conductivity, the vapor bubbles bombardment during the bubble formation by suspended nanoparticles, increase vapor movement and reduce the drag force due to Lorentz force, release the bubbles which accumulated on the inner wall of evaporator, reduce temperature fluctuation in the evaporation section, evaporator surface condition changing and finally occurring critical heat flux a shorter time.

Nomenclature: B, Magnetic field strength (Tesla); C_p, specific heat ($Jkg^{-1}K^{-1}$); d, thermosyphon diameter (m); E, error; I, electrical current (A); k, thermal conductivity ($Wm^{-2}°C^{-1}$); l, thermosyphon length (m); $\dot{m}$, coolant water mass flow rate (kgs^{-1}); Nu, Nusselt number; Q_{in}, inlet heat by evaporation (W); $Q_{net,\ cond}$, net heat conduction (W); $Q_{net,\ conv}$, net heat convection (W); Q_{out}, outlet heat by condensation (W); R, thermal resistance of thermosyphon ($W°C^{-1}$); T, Tesla; T_c, condenser temperature (K); T_e, evaporator temperature (K); T_i, inlet temperature of cooling water (K); T_o, outlet temperature of cooling water (K); TPCT, two-phase closed thermosyphon; V, electrical voltage (v); $\Delta\theta$, temperature difference of condensation and vaporization section (= T_e - T_c) (K); η_{th}, thermal efficiency of heat pipe.

REFERENCES

Bai B, Yabe A, Wakayama NI (1999). Quantitative analysis of convection flow of nitrogen gas and air under magnetic field gradient. AIAA J., 37: 1538-1546.

Braithwaite D, Beaugnon E, Tournier R (1991). Magnetically controlled convection in a paramagnetic fluid. Nature, 354: 667-673.

Chang YW, Cheng CH, Wang JC, Chen SL (2008). Heat pipe for cooling of electronic equipment. Energy Conversion Manag., 49: 3398-3404.

Choi SUS (1995). Enhancing thermal conductivity of fluid with nanoparticles, Developments and Applications of Non-Newtonian Flows. FED-V. 231/ MD-V, ASME, 66: 99-105.

Coursey JS, Kim J (2008). Nanofluid boiling, the effect of surface wettability. Int. J. Heat Fluid Flow. 29: 1577-1585.

Di Francescantonio N, Savino R, Abe Y (2008). New alcohol solutions for heat pipes: Marangoni effect and heat transfer enhancement. Int. J. Heat Mass Transf., 51: 6199-6207.

Duursma G, Sefiane K, Kennedy A (2009). Experimental Studies of Nanofluid Droplets in Spray Cooling. Heat Transfer Eng., 30(13): 1108-1120.

Fornalik E, Filar P, Tagawa T, Ozoe H, Szmyd S (2006). Effect of a magnetic field on the convection of paramagnetic fluid in unstable and stable thermosyphon-like configuration. Int. J. Heat Mass Transf., 49: 2642-2651.

Fukuzawa Y, Fuji Y (1978). Influence of Transverse Magnetic Field on Heat Transport Characteristics of Potassium Heat Pipe. J. Nuclear Sci. Technol., 15(10): 719-728.

Holman JD (1989). Experimental Methods for Engineers. Fifth ed. McGraw-Hill, New York.

Jeyadevan B, Koganezawa H, Nakatsuka K (2005). Performance evaluation of citric ion-stabilized magnetic fluid heat pipe. J. Magnetism Magnetic Mate., 289: 253-256.

Kaneda M, Tagawa T, Ozoe H (2002). Convection induced by a cusp-shaped magnetic field for air in a cube heated from above and cooled from below. J. Heat Transf., 124: 17-25.

Kang HU, Kim SH, Oh JM (2006). Estimation of thermal conductivity of nanofluid using experimental effective particle volume. Exp. Heat Transf., 19 (3): 181 - 191.

Kang SW, Wei WC, Tsai SH, Huang CC (2009). Experimental investigation of nanofluids on sintered heat pipe thermal performance. Appl. Therm. Eng. 29: 973–979.

Kang SW, Wei WC, Tsai SH, Yang SY (2006). Experimental investigation of silver nano-fluid on heat pipe thermal performance. Appl. Therm. Eng., 26: 2377-2382.

Khandekar S, Gautam AP, Sharma PK (2009). Multiple quasi-steady states in a closed loop pulsating heat pipe. Int. J. Therm. Sci., 48: 535-546.

Khandekar S, Joshi YM, Mehta B (2008). Thermal performance of closed two-phase thermosyphon using nanofluids. Int. J. Therm. Sci., 47: 659-667.

Kim HD, Moo JK, Kim H (2007). Experimental studies on CHF characteristics of nanofluids at pool boiling. Int. J. Multiphase Flow. 33: 691-706.

Kim J, Choi CK, Kang YT, Kim MG (2006). Effects of Thermodiffusion and Nanoparticles on Convective Instabilities in Binary Nanofluids. Nanoscale Microscale Thermophysical. Eng., 10(1): 29-39.

Kim SJ, Bang HC, Buongiorno J, Hu LW (2007). Surface wettability change during boiling of nanofluids and its effect on critical heat flux. Int. J. Heat Mass Transf., 50: 4105-4116.

Kulkarni DP, Namburu PK, Bargar HE, Das DK (2008). Convective Heat Transfer and Fluid Dynamic Characteristics of SiO_2 Ethylene Glycol/Water Nanofluid. Heat Transf. Eng., 29(12): 1027 - 1035.

Li C, Wang Z, Wang P, Peles Y, Koratkar N (2008). Nanostructured copper interfaces for enhanced boiling. Small. 4: 1084-1088.

Lin, YH, Kang SW, Chen HL (2008). Effect of silver nanofluid on pulsating heat pipe thermal performance. Appl. Therm. Eng., 28: 1312-1317.

Maki S, Tagawa T, Ozoe H (2002). Enhanced Convection or Quasi-Conduction States Measured in a Super-Conducting Magnet for Air in a Vertical Cylindrical Enclosure Heated From Below and Cooled From Above in a Gravity Field. J. Heat Transf., 124: 667-778.

Mikic BB, Rohnesow WM (1969). A new correlation of pool-boiling data including the effect of heating surface characteristics. J. Heat Transf., 91: 245-250.

Naphon P, Thongkum D, Assadamongkol P (2009). Heat pipe efficiency enhancement with refrigerant–nanoparticles mixtures. Energy Conversion Manage., 50: 772-776.

Narayan GP, Anoop KB, Das SK (2007). Mechanism of enhancement/deterioration of boiling heat transfer using stable nanoparticles suspension over vertical tubes. J. Appl. Phys., 102: 074317.

Noie SH (2005). Heat transfer characteristics of a two-phase closed thermosyphon. Appl. Therm. Eng., 25: 495-506.

Noie SH, Zeinali Heris S, Kahani M, Nowee SM (2009). Heat transfer enhancement using Al_2O_3/water nanofluid in a two-phase closed thermosyphon. Int. J. Heat Fluid Flow, 30: 700-705.

Quaresma JN, Macedo EN, DA Fonesca, HM, Orlande HRB, Cotta RM (2010). An Analysis of Heat Conduction Models for Nanofluids. Heat Transfer Eng., 31(14): 1125-1136.

Salehi H, Zeinali Heris Z, Noie SH (2011). Experimental study of two-Phase closed thermosyphon with nanofluid and magnetic field effect. J. Enhanced Heat Transf., 18(3): 261-269.

Tohver V, Chan A, Sakurada O, Lewis JA (2001). Nanoparticle engineering of complex fluid behavior. Langmuir. 17: 8414-8421.

Tseng WJ, Wu CH (2002). Aggregation, rheology and electrophoretic packing structure of aqueous Al_2O_3 nanoparticle suspensions, Acta Materialia, 50: 3757- 3766.

Wasan DT, Nikolov AD (2003). Spreading of nanofluids on solids. Nature, 423: 156-159.

Wen D (2008). Mechanisms of thermal nanofluids on enhanced critical heat flux (CHF). Int. J. Heat Mass Transf., 51: 4958-4965.

Yang H, Khandekar S, Groll M (2009). Performance characteristics of pulsating heat pipes as integral thermal spreaders. Int. J. Therm. Sci., 48: 815-824.

Yu W, France DM, Routbort JL, Choi SUS (2008). Review and Comparison of Nanofluid Thermal Conductivity and Heat Transfer Enhancements. Heat Transfer Eng., 29(5): 432-460.

Zeinali Heris S, Etemad SGh, Nasr Esfahany M (2009). Convective Heat Transfer of a Cu/Water Nanofluid Flowing Through a Circular Tube. Exp. Heat Transf., 22: 217-227.

Zeinali Heris S, Nasr Esfahany M, Etemad SGh (2007). Numerical Investigation of Nanofluid Laminar Convective Heat Transfer through a Circular Tube. *Numerical Heat Transfer Part A,* 52: 1043-1058.

Zhu D, Wu S, Wang N (2010). Thermal Physics and Critical Heat Flux Characteristics of Al_2O_3/H_2O Nanofluids. Heat Transf. Eng., 31(14) 1213-1219.